Космічна наука і технологія. ДОДАТОК. 2001. Т 7. № 2. С. 105—109.

UDC 524.7

THE DIFFUSION MODEL OF EXTRAGALACTIC RADIO SOURCE EXTENDED COMPONENTS

F. M. Kolesnikov

Institute of Radio Astronomy NANU, Kharkov, Ukraine
koles@ira.kharkov.ua

INTRODUCTION

The diffusion model is applied to extragalactic radio source extended components for modelling of radio source component images. It is assumed that the radio source hot spots (injection regions) are sources of relativistic electron plasma (accelerated by shocks). Electrons of plasma propagate due to the diffusion, lose the energy because of the synchrotron emission, and form the lobes (radio emitting clouds). The motions of the injection regions are introduced and it naturally explains the lobes size asymmetry and the displacement of the hot spots with respect to the center of the lobes [8]. There is the kinetic equation to be considered. The kinetic equation describes the diffusion of plasma relativistic electrons analytically and synchrotron losses are taken into account. The injection spectrum of the hot spots is taken as the power-law dependence on the energy within the given energy interval, the diffusion coefficient and the magnetic field are assumed to be dependent on coordinates. From the transfer equation the radio emission of electrons is found numerically, the reabsorption being taken into account. The Stoks parameters for plasma electrons are found from the formulas for the synchrotron emission. Velocities of the radio source hot spots and the diffusion velocity of plasma electrons determine the correlation of transverse and longitudinal lobe sizes. Observed changes of lobes at various frequencies accord with the diffusion model [3]. The reabsorption in the lobes leads to their asymmetry, depending on source rotation relative to the line of sight [6]. The distributions on a source of the polarized emission intensity, radio images at various frequencies and sources' spectra are received. The results are compared with the centimeter and decameter wavelengths observational data.

DIFFUSIONAL MODEL

The distribution function $N(E, \mathbf{r}, t)$ for the relativistic electrons satisfies the kinetic equation with a moving source:

$$\frac{\partial N}{\partial t} - \frac{\partial}{\partial E}(\beta E^2 N) - D\Delta N = Q\delta(x - Vt)\delta(y)\delta(z)E^{-\gamma_0}\Theta(t)\Theta(E_2 - E)\Theta(E - E_1).$$

The second term in the equation describes the synchrotron and the Compton losses with the synchrotron losses factor: $\beta = \left(\frac{32\pi}{9}\right)\left(\frac{e^2}{mc^2}\right)\frac{\omega_H + \omega_r}{m^2c^3}$, where $\omega_H + \omega_r$ is the energy density of the magnetic field and the emission. To simplify the model, disregard the possible coordinate dependence of the diffusion coefficient D, and the magnetic field H, the power-law dependence on the energy is taken for the diffusion coefficient: $D = D_0(E/E_D)^{\mu}$. The right-hand part of the kinetic equation corresponds to the point source of relativistic electrons (the hot spot) moving along the x-axis with the velocity V; the injection spectrum is taken as the power-law dependence on the energy $E^{-\gamma_0}$ in the range $E_1 < E < E_2$ and zero outside it. Here γ_0 is the injection index corresponding to acceleration in shocks ($\gamma_0 = 2$ in our calculations). The expression for the distribution function is given in the appendix. The Stoks parameters

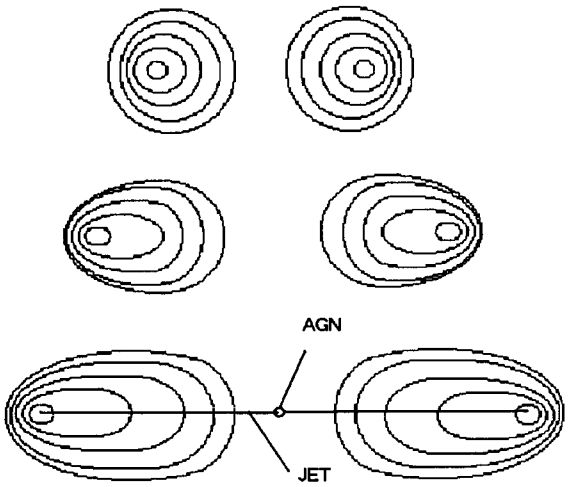

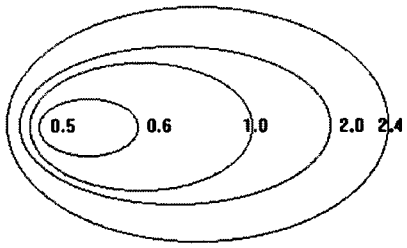

Figure 1. Radio source images for various correlations of hot spot velocity in the mapping plane and the electron diffusion velocity: $V/V_{\text{diff}} = 1, 4, 8$. $\gamma_0 = 2$; contour levels are 2, 4, 6, 8, 10 dB

Figure 2. The distribution of the spectral index α; $V/V_{\text{diff}} = 8$, $\gamma_0 = 2$; every contour conforms to a particular spectral index: 0.5, 0.6, 1.0, 2.0, 2.4

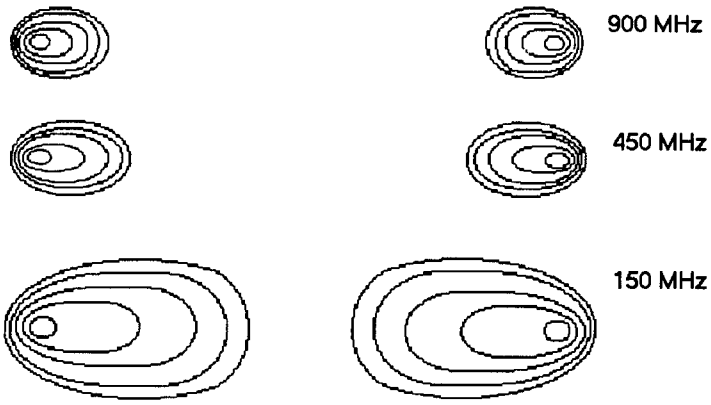

Figure 3. Radio source images obtained at three frequencies: 150 MHz, 450 MHz, 900 MHz; $\gamma_0 = 2$, $V/V_{\text{diff}} = 8$; contour levels are 2, 4, 6, 8 and 10 dB

for electrons are found from the formulas for the synchrotron emission [4], [5]:

$$I_\nu = I(\nu, \mathbf{r}, t) = \frac{\sqrt{3}e^3}{mc^2} \int dEdRN(E, \mathbf{r}, t) H \sin\chi \frac{\nu}{\nu_c} \int_{\nu/\nu_c}^{\infty} K_{5/3}(\eta) d\eta,$$

$$Q_\nu = Q(\nu, \mathbf{r}, t) = \frac{\sqrt{3}e^3}{mc^2} \int dEdRN(E, \mathbf{r}, t) H \sin\chi \cos 2\tilde{\chi} \frac{\nu}{\nu_c} K_{2/3}(\nu/\nu_c),$$

$$U_\nu = U(\nu, \mathbf{r}, t) = \frac{\sqrt{3}e^3}{mc^2} \int dEdRN(E, \mathbf{r}, t) H \sin\chi \sin 2\tilde{\chi} \frac{\nu}{\nu_c} K_{2/3}(\nu/\nu_c).$$

$\int dR$ ... corresponds to the integration along the line of sight, χ is the angle between the magnetizing force and the line of sight, $\tilde{\chi}$ is the angle between the mapping plane projection of the magnetic field H_{plane} and the biggest axis of the electric vector oscillation ellipse, ν_c is the cyclotron frequency: $\nu_c = = \frac{3eH_{\text{plane}}}{4\pi mc}\left(\frac{E}{m}\right.$

As to parameter V_ν it turns out to be zero in the ultrarelativistic approach. Figures 1—4 show examples

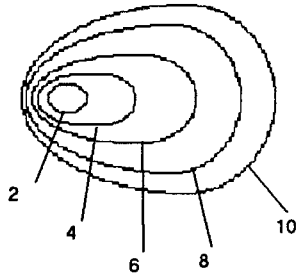

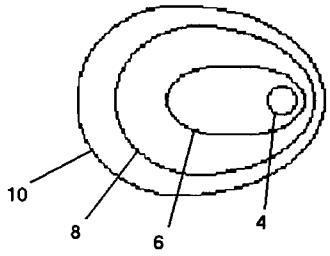

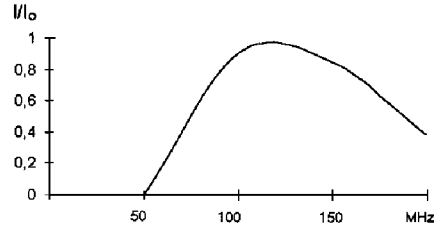

Figure 4. Images of radio source at 150 MHz rotated at 10 degrees (the left-hand lobe is closer to the observation point). The reabsorbtion is taken into account; $\gamma_0 = 2$, $V/V_{\text{diff}} = 8$; contour levels are 2, 4, 6, 8 and 10 dB

Figure 5. The radio source (the right-hand component, figure 4) spectra with account of reabsorption

of radio images for various values of parameters, reabsorption and the distribution of the spectral index are taken into account. Another example is the spectrum of a source with the reabsorption (figure 5). The spectrum has a typical abatement at low frequencies.

3C286

3C286 (1328+307) is a powerful radio source identified as a quasar at $z = 0.849$ [2]. The radio source has a steep spectrum which turns over at about 100 MHz. Subarcsecond resolution radio images show a misaligned triple structure, the central component of which accounts for at least 95 % of the total flux density at all frequencies. 3C286 is one of the strongest extragalactic sources in polarized emission (0.84 Jy at 5 GHz and 1.41 Jy at 1.4 GHz) and with a rotation measure close to zero. Hence, the observed orientation of the electric field vector is essentially independent of frequency. The polarized image reveals strong linear polarization, with the magnetic field which has dominant component which is perpendicular to the source axis (Fig. 6a). The former interpretation of the morphology of 3C286 was

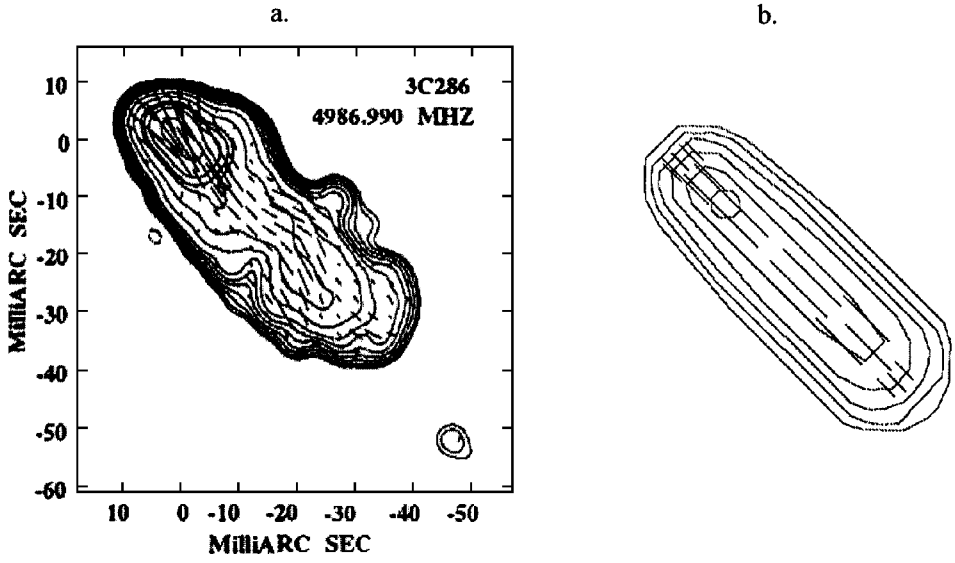

Figure 6. a: EVN polarizaton image of 3C286 [2], contour levels are −3.0, 3.0, 4.2, 6, 8.4, 12, 16.8, 24, 45, 90, 180, 240, 360, 750 mJy/beam and the peak is 1.0 Jy/beam; the vectors represent the projected orientation of the electric vector; their length is proportional to the polarized flux density; b: polarization image at 5000 MHz obtained in the diffusion model, contour levels are 2, 4, 8, 12, 16, 20 dB

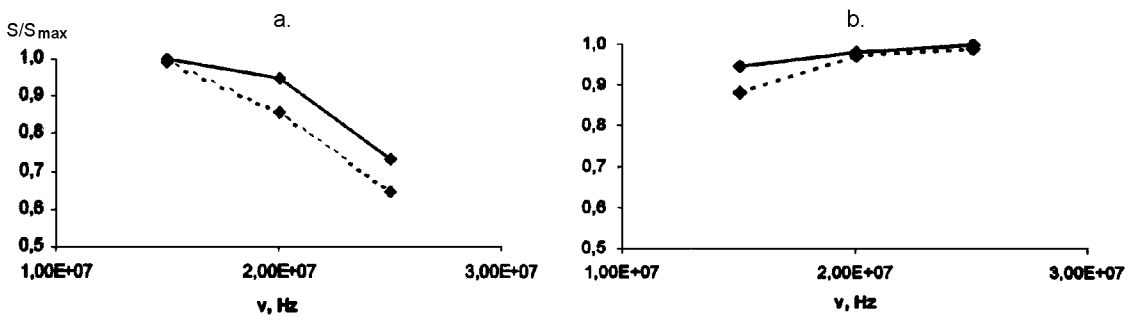

Figure 7. 3C196 components' spectra; a: the extended component spectrum; b: the compact component spectrum; dash lines correspond to the observation data and solid lines are model curves

that the brightest region of 3C286 harbours the core, and the overall arcsecond morphology is that of a misaligned, asymmetric and core-dominated triple. However, on mas scales the cores of quasars are rarely strongly polarized (at most 2 %) and the magnetic fields in the jets of quasars are often quite closely parallel to the jet axes. Moreover, the lack of reported significant variability in the total flux density of 3C286 implies that the source orientation is near the plane of the sky and that the core has a steep high frequency spectrum. There is the possibility that the brightest region of 3C286 is a lobe with the hot-spots in an asymmetric, compact FR II radio source. A steep radio spectrum, high fractional polarization and the perpendicular field orientation are in agreement with the observed properties of the hot-spot regions of FR II sources, where the high polarization and transverse field are originated by a compression shock. The strong asymmetry between the sizes and flux densities of the two lobes may be due to different local environments, and the main lobe would apper brighter and smaller due to a stronger confinement of the radio emitting plasma. It was obtained a polarization image of the 3C286 southwest component at 5 GHz in the model numerically (Fig. 6b).

3C196

3C196 (z = 0.871) is one of the brightest radio source of the south sky. At high frequencies the 3C196 radio images commonly consist of two compact components. The angular structure study of the radio emission was carried out by URAN-1 and URAN-4 radio interferometers at 25, 20 and 16.7 MHz [7]. As it has been found the angular structure at high frequencies and at decameters were noticeably different. Only one compact component was observable at decameters and an extended component was detected. At three frequencies (25, 20 and 16.7 MHz) the extended and compact component fluxes and spectral indexes (between 25 and 20 MHz) were obtained. In the diffusion model network we computed component spectra and spectral indexes. The extended component spectral index is 1.14 (1.25 is observed) and −0.08 for the compact component (−0.08 is observed).

APPENDIX

The distribution function $N(E, \mathbf{r}, t)$:

$$N(E, \mathbf{r}, t) = \frac{Q_0 E^{-2}}{8\pi^{3/2}\beta}\left(\frac{\beta(1-\mu)E_D^{\mu}}{D_0}\right)^{\{}(\gamma_0 - 1)(1-\mu)(1-\mu)\times$$

$$\times \int_{\lambda^2(E_2)}^{\lambda^2(E)} \frac{d\lambda_0^2 \lambda_0^{2(\gamma_0-1)(1-\mu)-2}}{(\lambda^2-\lambda_0^2)^{3/2}} \Theta[tD_0-(\lambda^2-\lambda_0^2)] \exp\left\{\frac{-\left[x-V*t+\frac{v}{D_0}(\lambda^2-\lambda_0^2)\right]^2-y^2-z^2}{4(\lambda^2-\lambda_0^2)}\right\}.$$

In this expression for the distribution function $\lambda^2 = D_0 E^{\mu-1}/(1-\mu)E_D^{\mu}\beta)$ is the square of the diffusion length [1]. We see from expressions for the distribution function and the radio spectrum (4) that the external shape of radio lobes is determined by the relation between the electron diffusion velocity $V_{diff} = = D_0/\lambda$ and the velocity of the source V in the mapping plane.

REFERENCES

1. Berezinskiy V. S., Bulanov S. V., Ginzburg V. L., et al. Astrophysics of cosmic rays. — Moscow: Nauka, 1984.—358 p.
2. Dallacasa D., Schilizzi R. T., Sanghera H. S., et. al. 5GHz EVN polarization of 3C286. Extragalactic radio sources // IAU.—1996.—**175**.—P. 85-87.
3. Gestrin S. G., Kontorovich V. M., Kochanov A. E. The diffusion model of extended radiocomponents and jets with the moving source of accelerated particles // Kinematica i Fizika Nebesnykh Tel.—1987.—**3**, N 4.—P. 57—67.
4. Ginzburg V. L. Theoretical Physics and Astrophysics. — Moscow: Nauka, 1987.—488 p.
5. Ginzburg V. L., Syrovatskii S. I. Origin of cosmic rays. — Moscow: Nauka, 1963.—384 p.
6. Kontorovich V. M., Kolesnikov F. M. The images of extragalactic radio sources in the diffusion model // Gamov Memorial International Conference.—1999.—**45**.—P. 87—89.
7. Men' A. V., Braude S. Ya., Rashkovskij N. K., et al. Radio emission of the quasar 3C196: the angular structure // Izvestiya Vysshikh Uchebnykh Zavedeniy, Radiofizika.—1990.—**33**, N 5.—P. 523—533.
8. Valtaoja E. Diffusion of electrons in radio galaxies // Astron. and Astrophys.—1982.—**111**, N 2.—P. 213—219.